Effects of crustal fields on the Martian ionosphere as seen by MAVEN

1. Introduction

The goal of the proposed work is to understand how crustal fields influence the density, temperature, composition, and electrodynamics of the Martian ionosphere. This will be achieved primarily through analysis of data from NASA's Mars Atmosphere and Volatile Evolution (MAVEN) mission, along with modeling work to facilitate the interpretation of MAVEN data.

Mars is unique among the terrestrial planets because it lacks a global intrinsic magnetic field but possesses regions of strong crustal magnetic field that are concentrated in the southern hemisphere. For example, Figure 1 shows global magnetic field maps of Mars produced using data from Mars Global Surveyor (MGS) at 400 km altitude [*Connerney et al.*, 2001]. The crustal magnetic fields are primarily radial in direction, with magnitudes up to several hundred nanoTesla (nT) at 400 km altitude, and are strongest at southern latitudes and longitudes ~120º-240º. These crustal fields are important because they affect the structure of the ionosphere [e.g. *Withers et al.*, 2005; *Nielsen et al.*, 2007] and can influence the interaction between the planet and the solar wind [e.g. *Mitchell et al.* 2001; *Edberg et al.*, 2008], which can have implications for atmospheric escape.

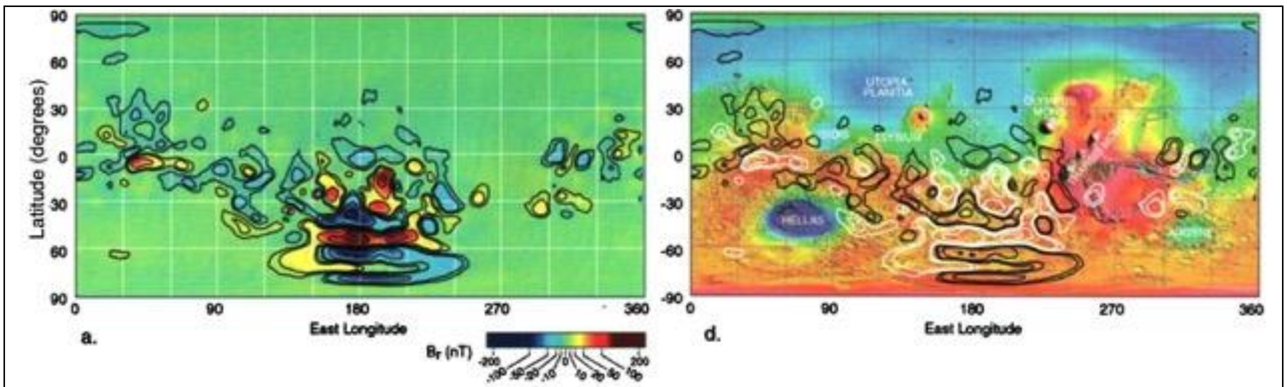

Figure 1. (left) Radial magnetic field at 400 km altitude. (right) Contours of |B| = 10, 20, 50, 100, 200 nT overlaid on MOLA topography. From *Connerney et al.* [2001], Figure 1.

The influence of crustal fields on the Martian environment is an area of active research through observational studies of MGS and Mars Express (MEX) data and complementary modeling work [e.g. *Matta et al.*, 2015]. Observations have shown that the presence of strong crustal field affects the structure of the ionosphere on global scales and that the crustal magnetic field orientation can strongly influence the local ionospheric structure. An example of the effect of crustal fields on global scales is shown in Figure 2. *Andrews et al.* [2015a] compared electron densities above 300 km from the MARSIS radar sounder instrument on MEX to an empirical model of the Martian ionosphere and found that the measured values exceeded the model predictions in regions of strongest crustal fields (see Figure 2 and compare to regions of strong crustal magnetic field in Figure 1). More recently, MAVEN observations have also been used to study the influence of crustal fields on ionospheric electron densities. For example, *Andrews et*

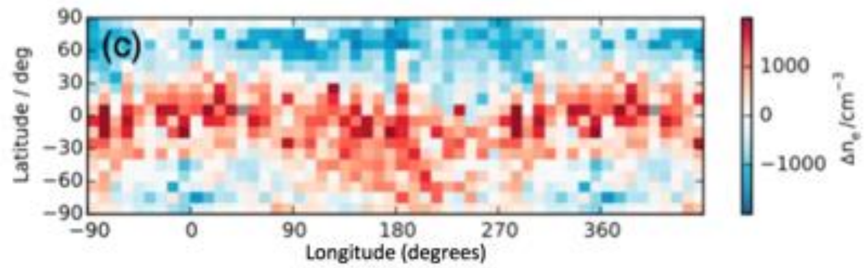

Figure 2. Difference between the electron density measured with MEX and an empirical model [*Němec et al.*, 2011]. From Figure 3 of *Andrews et al.* [2015a].

al. [2015b] presented initial MAVEN measurements from the Langmuir Probe and Waves (LPW) instrument that showed that the orbit-to-orbit variability in the electron density is largest and positive in regions of strong crustal magnetic field, suggesting enhanced electron densities in those regions.

Observations have also shown local crustal field effects on the ionospheric structure that are typically associated with a strongly vertical magnetic field orientation. For example, MGS radio occultation electron density profiles from regions of strong crustal fields have been shown to have localized "bite-outs" [*Withers et al.*, 2005]. *Nielsen et al.* [2007] reported enhanced peak electron densities in magnetic cusps, or regions of strongly vertical magnetic field that are likely open to the solar wind. The peak electron density is the maximum electron density in an electron density altitude profile and is typically located at ~120-130 km altitude at the subsolar point. The left panel of figure 2 shows examples of normal (141) and enhanced (132) electron density profiles and the right panel of Figure 3 shows MEX's orbital ground tracks, with regions of the enhanced electron densities plotted with white '+' symbols. *Nielsen et al.* [2007] suggested that the electron density enhancement was due to plasma heating by the two-stream plasma instability driven by the solar wind induced electric field. They concluded "[cusp] magnetic fields can reach further into the solar wind than field lines from other regions, an indication that the solar wind interaction with the crustal fields plays a role in forming the events." Similarly, *Gurnett et al.* [2008] proposed that electron density "bulges" observed with MEX could be "caused by solar wind electrons that have access to the lower levels of the ionosphere along nearly vertical open magnetic field lines. The resultant electron heating increases the plasma scale height and electron density of the ionosphere in these regions, thereby accounting for the density bulges."

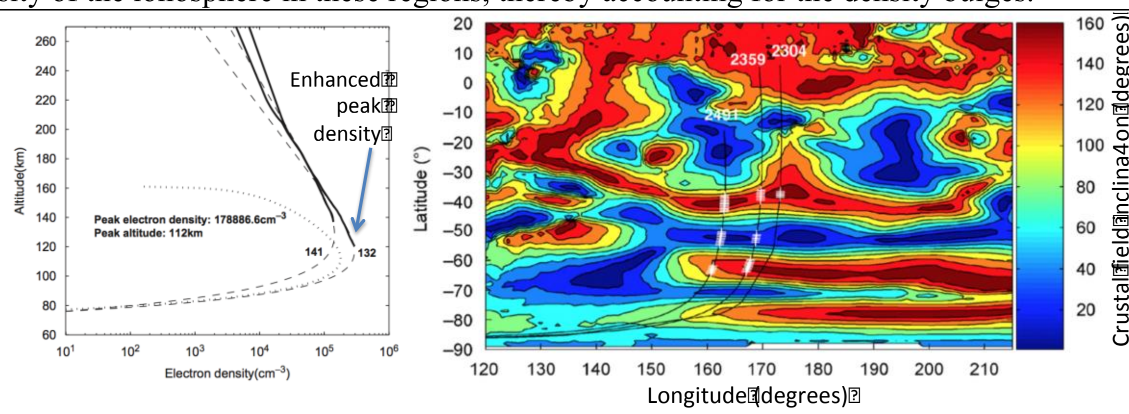

Figure 3. (left) Electron density profiles outside (141) and inside (132) a magnetic cusp. (right) Orbital ground tracks (black lines) and locations of enhanced peak n_e (white '+' symbols) overlaid on a map of the magnetic field inclination. Enhanced peak densities occur where the field is strongly vertical. Modified from Figures 2 and 5 of *Nielsen et al.* [2007].

Modeling efforts using global MHD models have largely focused on how crustal fields influence the solar wind interaction with the planet [e.g. *Ma et al.*, 2002]. *Fillingim et al.* [2012] used an electron transport model to show that electron densities in the nightside ionosphere can be enhanced in cusp regions due to ionospheric electrojets, or currents, driven by neutral winds. They predicted that the magnetic signatures of the electrojets would be ~10 percent of the field magnitude and would be observable below 400 km. Similarly, *Riousset et al.* [2014] used a multifluid MHD model to study the electrodynamics in a magnetic cusp at Mars. They found smaller ion fluxes (O_2^+ and CO_2^+) in magnetic loops than in cusp fields at 300 km altitude and suggested this was because the open cusp field lines allowed ions to flow upward from the lower regions of the ionosphere and possibly to eventually escape. More recently, *Matta et al.* [2015] used a 2-D fluid model of the Martian ionosphere to study field-aligned vertical and horizontal plasma transport in regions of strong crustal fields. They showed that regions of strongly vertical crustal field feature an "inflated" ionosphere with enhanced electron densities compared to regions of strongly horizontal fields above 150 km and that these effects can be observed "without including solar wind plasma interactions, electron precipitation, plasma temperature effects upon chemistry, wave dissipation effects, or transport by neutral winds."

These earlier studies using MGS and MEX data or models have established the importance of crustal magnetic fields on the structure of the Martian ionosphere, though there are still some important unanswered questions about the underlying physical processes at play. This is due in part to the fact that many of these earlier observational studies were limited by incomplete measurements or orbital coverage. **We propose to use data from NASA's Mars Atmosphere and Volatile Evolution (MAVEN) mission, along with complementary modeling work, to investigate how crustal fields influence the structure of the dayside Martian ionosphere.** MAVEN data provide the best opportunity to date to study the effects of crustal magnetic fields on the Martian ionosphere because they are the first to include comprehensive plasma and magnetic field measurements and <u>the first measurements of the electron temperature and ionospheric composition since Viking</u>. Ionospheric models of diurnal changes in electron density have been limited by a lack of information regarding the variability of ion and electron temperatures [e.g. *Fox*, 2004; *Mendillo et al.*, 2011; *Fallows et al.*, 2015]. Electron temperatures are important to the electron density because the dissociative recombination coefficient for the most abundant ion (O_2^+) in the Martian ionosphere is proportional to $T_e^{-0.7}$ [*Schunk and Nagy*, 2009].

Through data analysis and modeling we will answer the following questions:

- ***How do the composition, density, and temperature of the dayside Martian ionosphere change in regions of strong crustal field?***
- ***What processes lead to enhanced electron densities in cusp fields?***

The data analysis effort will include both detailed case studies of local crustal field effects and global, long-term surveys. We will consider the effects of the crustal field magnitude and direction as well as its topology. By "topology" we mean whether a crustal field line is "closed" and has both ends rooted in the planet or "open" and has one end in the solar wind, while by field direction we are referring to the orientation of the magnetic field (i.e. is it horizontal or vertical). We will focus on the dayside ionosphere, which is less variable than the nightside ionosphere and where other sources of variability due to spatial (e.g. solar zenith angle) and temporal (e.g. solar ionizing flux) have been studied in detail and can easily be predicted and quantified [e.g. *Withers*, 2009].

2. MAVEN data to be used in the proposed work

NASA's MAVEN mission launched in 2013 and entered Mars orbit in September 2014. For MAVEN's one year primary science mission, which began in November 2014, the spacecraft was located in a 4.5 h elliptical orbit around Mars, with periapsis typically at ~150 km, apoapsis at ~6200 km, and a 75° inclination [*Jakosky et al.*, 2015]. The primary science mission included four "deep dip" intervals (February, April, July, and September 2015) in which periapsis was lowered to ~120-130 km for about a week. MAVEN data through April 2016 are publicly accessible through the PDS.

MAVEN provides the best opportunity to date for studying the effects of crustal fields on the Martian ionosphere. Earlier missions like MGS and MEX provided crucial information that led to the discovery of crustal fields and established that these crustal fields influence the structure of the Martian ionosphere, but studies from these earlier missions were limited by the spacecraft instrumentation and/or orbital effects. For example, MGS radio occultation profiles of the electron density are limited in their altitude coverage, typically extending only as high as ~200 km, and Mars Express lacked a magnetometer, hindering the measurement of the local magnetic field and ionospheric currents. Prior to MAVEN, the only electron temperatures measured in the Martian ionosphere came from a single profile from the Viking lander that extended only as low as ~200 km [*Hanson and Mantas*, 1988]. The electron temperature measurements are crucial for determining the processes by which crustal fields influence the structure of the ionosphere, for example by testing the suggestion that electron densities in cusp regions are enhanced due to plasma heating by the solar wind [e.g. *Nielsen et al.*, 2007]. MAVEN data also provide *in situ* measurements of the crustal field effects on the lower ionosphere, unlike MGS (remote radio occultation measurements for altitudes below 400 km) and MEX (remote radar sounding observations below ~275 km).

MAVEN includes a suite of particle and fields instruments that provide comprehensive measurements of the local magnetic field and plasma properties, and a Neutral Gas and Ion Mass Spectrometer (NGIMS) [*Mahaffy et al.*, 2014] that measures the ion composition in the ionosphere. In our proposed work we will use data from the following MAVEN instruments:

- NGIMS – measures neutral and ion densities with masses from 2 to 150 amu but does not measure protons
- LPW (Langmuir Probe and Waves, *Andersson et al.* [2015]) – measures electron densities ~100 cm^{-3} to 10^6 cm^{-3} and electron temperatures 500-50000 K at a 4-second time resolution
- MAG (Magnetic field investigation, *Connerney et al.* [2015]) – includes two magnetometers that measure the magnetic field components with a time resolution of 32 vector samples/second
- SWEA (Solar Wind Electron Analyzer, *Jakosky et al.* [2015]) – measures the density and velocity (pitch angle) distributions of electrons with energies from 5 eV to 5 keV
- SWIA (Solar Wind Ion Analyzer, *Halekas et al.* [2014]) – measures the density and velocity distributions of ions with energies from 5.1 eV to 26 keV
- STATIC (SupraThermal and Thermal Ion Composition, *McFadden et al.,* [2015]) – measures the composition and velocity of ions with energies from 0.1 eV to 30 keV
- EUVM (Extreme Ultraviolet monitor, *Eparvier et al.* [2015]) – measures the solar irradiance at soft x-ray and EUV wavelengths, but is pointed away from the Sun at periapsis. Therefore, to estimate the solar ionizing flux at Mars when measurements are unavailable we will use the EUVM level 3 data product, which is a modeled spectral irradiance based on a modified

version of the Flare Irradiance Spectral Model (FISM) [*Chamberlain et al.*, 2007, 2008] that can be applied to planetary targets other than Earth and incorporates measurements from MAVEN's EUVM. The modeled irradiances are available with a 1-minute time resolution and at wavelengths 0-190 nm.

3. Summary of proposed research

Our goal is to study the effects of crustal magnetic fields on the Martian ionosphere by analyzing MAVEN data in both detailed case studies and global, long-term surveys. The proposed research is comprised of 3 tasks. **Task A** is a case study of data from a few dozen MAVEN orbits that passed through regions of strong crustal fields, including cusp regions that may be open to the solar wind. **Task B** is a global survey of the effects of crustal field magnitude, direction, and topology on ionospheric properties like the electron density, electron temperature, and ionospheric composition. **Task C** uses the BU Mars Ionosphere Model to interpret the results of Tasks A and B.

3.1 Task A: Case studies of MAVEN data from crustal field regions

The goal of the work proposed in this Task is to use MAVEN observations to characterize the magnetic field and plasma environment in cusp magnetic field regions and establish what physical processes influence the ionospheric structure in these regions. We propose to conduct a case study of a few dozen MAVEN orbits from the fall of 2015, when MAVEN's orbit was ideal for studying the effects of crustal magnetic fields on the dayside ionosphere: orbital periapsis was on the dayside at afternoon local times, and the spacecraft was located in the southern hemisphere at most ionospheric altitudes. For example, Figure 4 shows MAVEN's location during the inbound portion of the 2-9 September 2015 deep dip orbits. Several of these orbits passed directly through regions of strongly vertical crustal field (e.g. compare to the *Nielsen et al.* [2007] figure reproduced here as Figure 2). Periapsis was at ~125 km altitude and ~80º SZA, at the southern edge of each orbital segment in Figure 4. About 200 MAVEN orbits from late August to late September had a similar geometry.

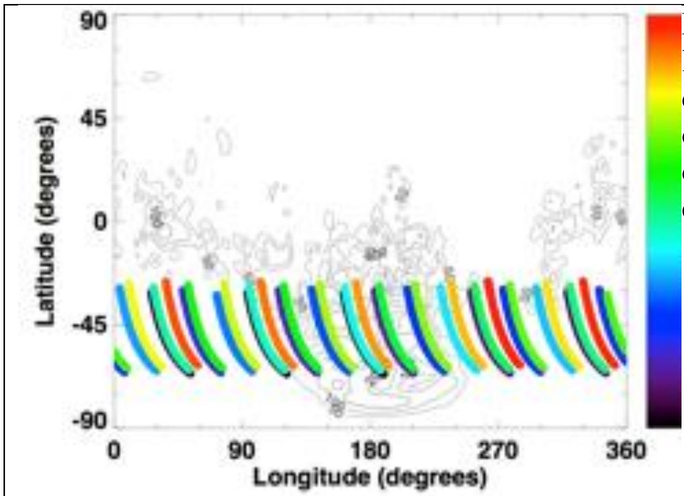

Figure 4. MAVEN's location (alt. < 400 km) during the deep dip orbits in Sept. 2015, overlaid on modeled contours of crustal field [*Cain et al.*, 2003].

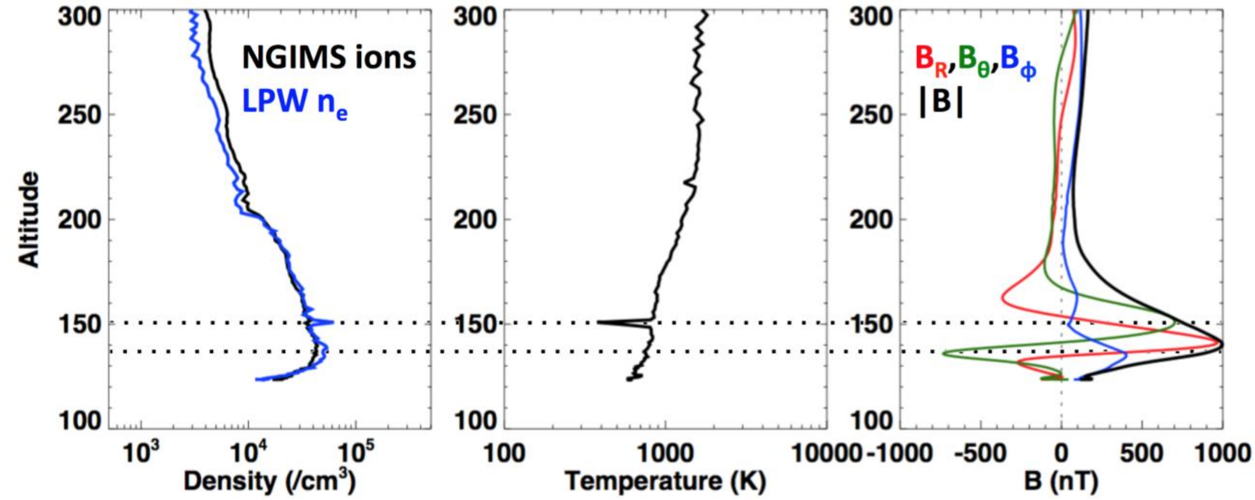

Figure 5. Altitude profiles of ionospheric properties measured by MAVEN during orbit 1822 inbound in a region of strong crustal magnetic fields. (right) LPW electron density and NGIMS ion density. (middle) LPW electron temperature. (left) MAVEN magnetic field measurements.

A preliminary analysis of MAVEN data from these regions shows that the LPW electron density profiles show consistent fluctuations when the spacecraft passes through certain regions. An example from orbit 1822 is shown in Figure 5. The horizontal dashed lines highlight two enhancements of the LPW electron density n_e (blue line in left panel) relative to the total ion density measured by NGIMS (black), which should be equal to the electron density under the expected photochemical equilibrium conditions. Both n_e enhancements occur when the radial magnetic field (red line in right panel) goes through zero, indicating a strongly horizontal magnetic field. At the same altitude we observe small "kinks" in the azimuthal magnetic field component (blue line in right panel), indicating currents, measured by MAVEN. At the same altitude as the top n_e enhancement the electron temperature T_e decreases sharply from ~800 K to ~400 K (middle panel). Interestingly, there does not appear to be any perturbation in n_e or T_e in the regions of strongly vertical magnetic field, contrary to the observations of *Nielsen et al.* [2007].

About a dozen MAVEN orbits from fall 2015 passed through very similar regions as in the example from orbit 1822 (longitude ~180º-200º, southern hemisphere latitudes, altitude < ~250 km, solar zenith angle ~80º). In each case the electron density displayed consistent fluctuations every time the spacecraft passed through a region of strongly horizontal crustal magnetic field. In some cases the electron density was enhanced while in other cases it was depleted, and in some cases the NGIMS total ion density also fluctuated. Currents indicated by "kinks" in the magnetic field are observed in almost every additional orbit. Fluctuations (both enhancements and decreases) in the electron temperature are frequently, but not always, observed, and are almost all significantly smaller (maximum ~100 K) than the example shown in Figure 5.

Although the density perturbations occur at altitudes where the field lines are horizontal, not vertical, we believe these regions are magnetic cusps. Magnetic cusps are frequently associated with vertical field lines because vertical field lines are more likely than horizontal field lines to be open to the solar wind, since horizontal field lines can occur at the top of a closed magnetic loop, as shown in the cartoon in Figure 6 (left). A more accurate way to infer the topology of a magnetic field line, meaning whether the field lines are open or closed to the solar wind, is to examine the pitch angle distribution of particles on the field line. The pitch angle is the angle a particle makes with respect to the magnetic field direction. Open field lines feature more field-aligned pitch angle distributions, peaking at 0º or 180º. Closed field lines feature bouncing particles with "trapped" distributions that peak near 90º. An initial analysis of the pitch angle distribution measured by SWEA suggests that these horizontal field lines are open to the solar wind. At ~150 km altitude in orbit 1822 (Figure 5) the spacecraft was at ~84º SZA, so very close to the terminator, so it is possible that some open field lines are pulled anti-sunward by the solar wind, resulting in an open horizontal field line as illustrated in Figure 6 (right).

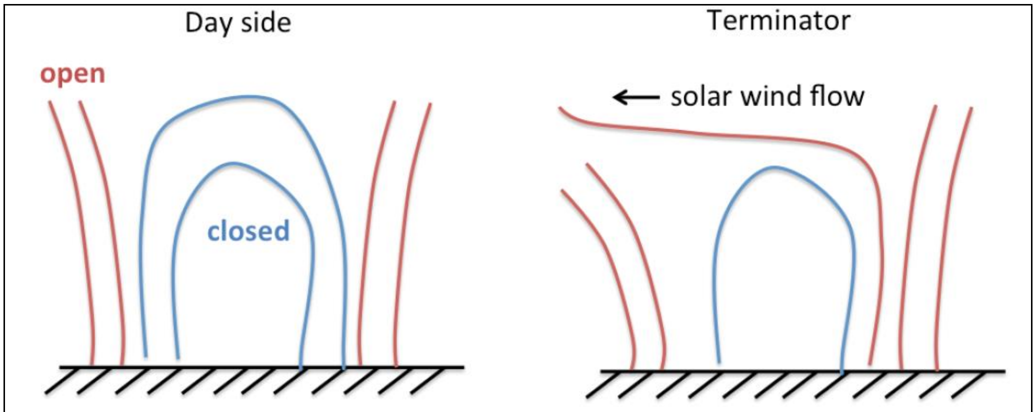

Figure 6. Cartoon illustrating the possible field line geometry from orbit 1822 (right).

We will characterize the magnetic field and plasma environment in magnetic cusp regions at Mars by analyzing MAVEN data from orbit 1822 and a dozen or so other orbits with similar orbital geometry. Specifically, we will:

- characterize the electron and ion density fluctuations (how frequently do we observe an enhancement vs. a depletion, and by what fraction does the density change?) in cusp regions
- determine the topology of the magnetic field to confirm that these horizontal field lines are open to the solar wind
- quantify changes in electron temperature in cusp regions (at altitudes where electron density fluctuations are observed) and, more generally, compare electron temperatures from nearly-consecutive orbits that passed over regions of weak and strong crustal fields, to look for evidence of plasma heating
- characterize the field geometry at the altitude of the electron density fluctuations and calculate the magnitude and direction of the currents
- examine the energy spectra measured by SWEA and SWIA to look for evidence of precipitating solar wind particles

Our goal with the work in Task A is to answer the question **what physical processes contribute to these electron density fluctuations?** As discussed earlier, electron density perturbations have been reported in magnetic cusps from both models and observations [e.g. *Nielsen et al.*, 2007], with the suggestion that the solar wind can penetrate the open field lines and heat the plasma in the ionosphere. Because electron temperature measurements are available for the first time, along with detailed electron energy and velocity distributions from SWEA, we can test this suggestion that penetrating solar wind particles heat the plasma in the ionosphere. We can also measure any field-aligned currents from the magnetic field measurements and ion velocity distributions with STATIC. If we do observe increases in the electron temperature near magnetic cusp regions, other MAVEN measurements may also help distinguish whether the plasma heating influences the electron density by reducing the dissociative recombination coefficient as suggested by *Nielsen et al.* [2007] or whether the heating affects the electron density by increasing the plasma scale height as proposed by *Gurnett et al.* [2008]. However, if we do not observe any changes in the electron temperature, that could instead suggest that the ionospheric structure is instead influenced by field-aligned vertical and horizontal transport without including solar wind plasma interactions, as modeled by *Matta et al.* [2015]. Complementary modeling work described in more detail in Task C will help us further investigate the role of field-aligned vertical and horizontal transport in influencing the structure and composition of the ionosphere.

Expected significance: The results of Task A will establish what physical processes influence the ionospheric structure in magnetic cusp regions. Specifically, because MAVEN provides the first electron temperature measurements since Viking we will be able to test whether electron densities are enhanced in cusp regions due to plasma heating by the solar wind or whether the changes in the ionospheric structure can be explained by field-aligned vertical and horizontal plasma transport alone. We anticipate publishing our findings in at least one paper in a peer-reviewed journal.

3.2 Task B: Global survey of crustal field effects on ionospheric properties

The second task will be a global survey of the LPW and NGIMS data to examine the effects of crustal magnetic fields on properties of the dayside ionosphere including the electron density, electron temperature, and ion composition. We will quantify how these ionospheric properties change in regions of strong crustal field and examine whether and how they are influenced by the magnetic field direction. While previous studies have examined the global effects of crustal fields on the ionosphere above ~300 km altitude [e.g. *Andrews et al.*, 2015a], MAVEN data provide the first opportunity to quantify these effects at lower altitudes.

Some initial work for this task has already been completed, as shown in Figures 7 and 8. Figure 7 presents an overview of LPW data in the dayside Martian ionosphere (SZA < 90º) as a function of Mars latitude and longitude at altitude 240-260 km (left) and 300-320 km (right), from October 2014 through April 2016. The strong crustal fields are confined to a few regions as discussed earlier (Figure 1), so an easy way to examine the influence of crustal fields on, for example, the electron density and temperature, is to see how these quantities vary with latitude and longitude.

The top panel of Figure 7 shows the number of data points in each 10º latitude by 10º longitude bin. Below 60º N latitude the data are relatively evenly distributed in latitude/longitude space, and at all altitudes 140-400 km (not shown) there are typically at least ~30 data points in each bin. This demonstrates that the MAVEN data through April 2016 provide sufficient spatial coverage to study how ionospheric properties vary with latitude and longitude, which is a proxy for how these properties change in response to regions of strong crustal fields. The middle and bottom panels of Figure 7 show the median electron density and temperature, respectively, in

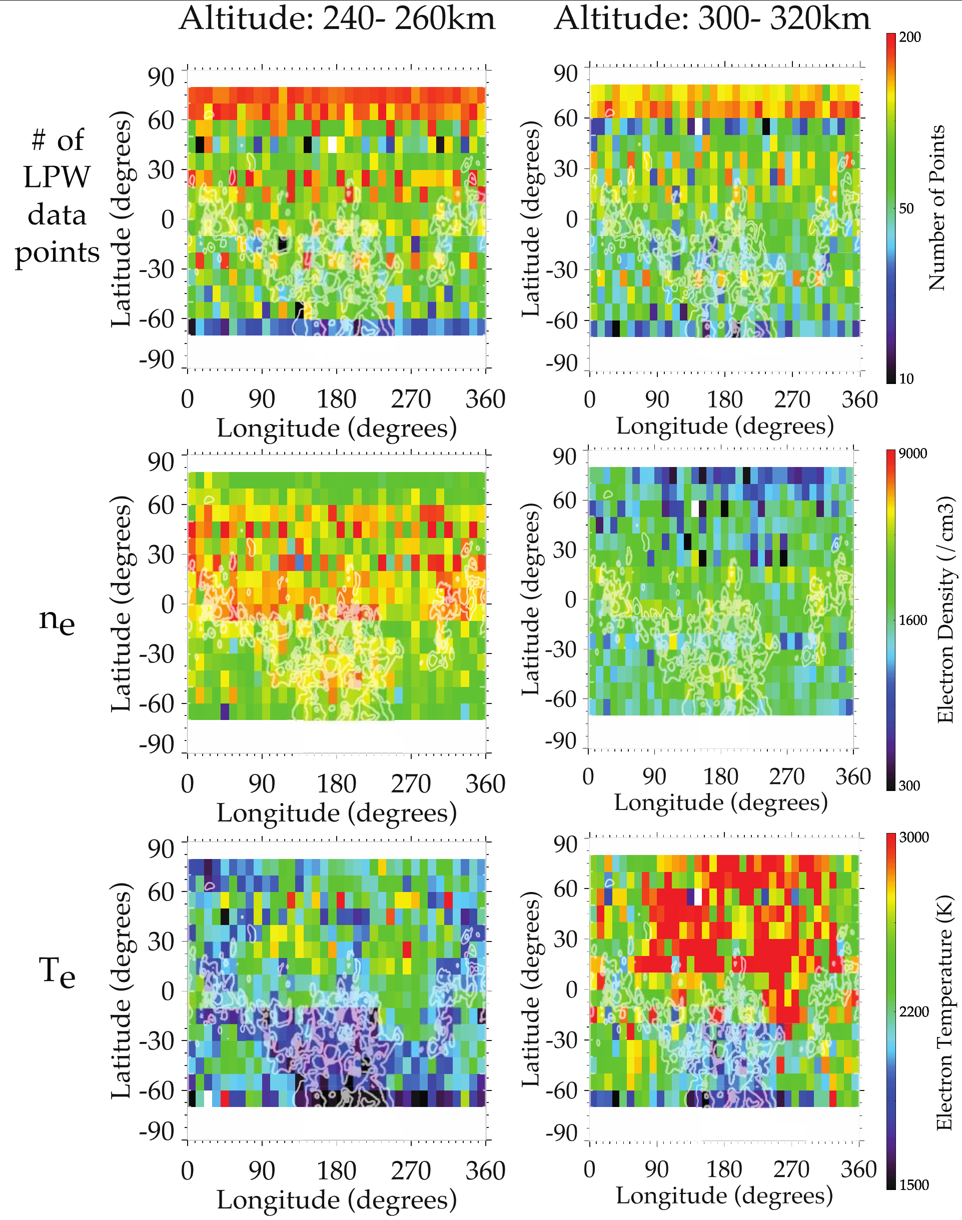

Figure 7. Overview of LPW data in the dayside Martian ionosphere as a function of Mars latitude and longitude, for altitude ranges 240-260 km (left column) and 300-320 km (right column). The top row shows the number of data points in each 10º latitude x 10º longitude bin. The middle row shows the median electron density in each bin. The bottom row shows the median electron temperature in each bin. Overlaid on each plot are contours of the Cain et al. [2003] crustal magnetic field model.

each bin. In regions of strong crustal magnetic fields at ~120º-240º longitude, n_e is enhanced and T_e is smaller, than in the other regions.

Similarly, Figure 8 shows median dayside electron density (left) and temperature (right) profiles measured by LPW in the southern hemisphere for four different longitude ranges. The green profiles correspond to longitudes 160º-180º, where the crustal field magnitude is strong. Above ~200 km the green profiles clearly stand out from the profiles at longitudes where the crustal fields are weak.

Together, the MAVEN data shown in Figures 7 and 8 suggest that the electron density and temperature measured by LPW are influenced by the proximity to regions of strong crustal fields. With regards to the electron density, this confirms the result of previous studies using MGS and MEX data [e.g. *Andrews et al.*, 2015a]. However, with regards to the influence of crustal fields on the electron temperature, this represents a completely new finding, since MAVEN's electron temperature measurements are the first since the single Viking profile.

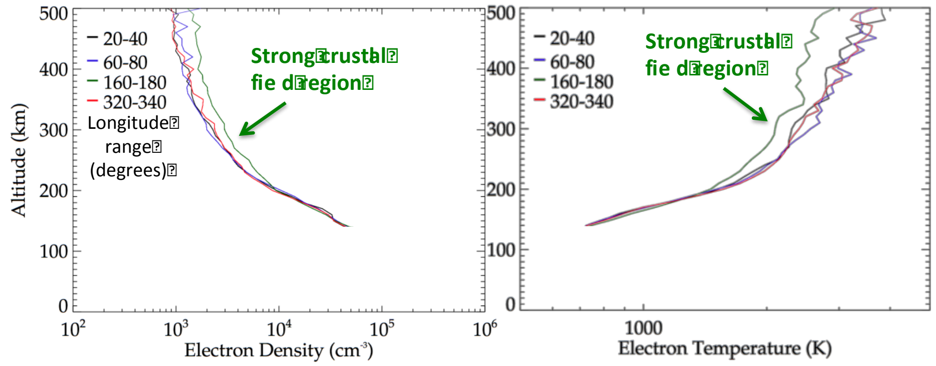

Figure 8. Median electron density (left) and electron temperature (right) profiles for 4 different longitude ranges as noted. All data are from the dayside southern hemisphere above 140 km.

For this task we will continue analyzing MAVEN data to quantify the effects of crustal fields on ionospheric properties, including the electron density and temperature as shown in our preliminary work, and will extend our analysis to examine the ion composition measured by NGIMS. We will produce maps similar to those in Figure 7 and 8 for the absolute and fractional abundances of various ion species, including O_2^+, O^+, CO_2^+, NO^+, HNO^+, and HCO^+. Electrons in the Martian ionosphere are mostly produced through photoionization of atmospheric CO_2, which produces a CO_2^+ ion that quickly recombines with atomic oxygen to produce O_2^+, the dominant ion in the lower ionosphere, and neutral CO [e.g. *Withers*, 2009]. Changes in the absolute or relative abundances of different ion species can provide insight into the processes by which crustal fields influence the ionospheric structure and atmospheric escape, since different ion species escape at different rates.

From the data used to create Figures 7 and 8 we can also produce scatter plots of the binned ionospheric properties as a function of the binned crustal field magnitude to better quantify the effects of the strong crustal fields. We will consider the influence of both the magnitude and orientation of the crustal magnetic field. Figures 7 and 8 demonstrate an influence on crustal field magnitude, but we will also perform similar analysis focusing on how ionospheric properties vary in regions of strongly vertical or strongly horizontal magnetic field using the magnetic field orientation measured by MAVEN.

The analysis in Figures 7 and 8 is very preliminary and does not account for possible temporal changes in the ionosphere due to Mars season, the Mars-Sun distance, changes in solar ionizing flux (measured with MAVEN's EUVM instrument), transient changes due to solar storms, etc. For example, in Figure 7 there appears to be a north-south hemispherical asymmetry in both n_e and T_e, which could be explained by seasonal variability. We will carefully control for these other sources of ionospheric variability when performing our analysis.

For the electron temperatures, we may also need to control for changes with solar zenith angle (SZA). We have assumed in Figures 7 and 8 that the electron temperature dependence on SZA is small, since the dayside electron density at Mars has been shown to change with SZA in a manner that is broadly consistent with photochemical theory [e.g. *Withers,* 2009]. At SZA < ~70° the changes in electron density with SZA are relatively small. *Withers et al.* [2014] used an analytical model to predict that electron temperatures will also display relatively small changes with small dayside SZA (< ~60°) at a given altitude. An important first step in our analysis will be to test this prediction and quantify how the electron temperature changes with SZA (and altitude). If we find that the electron temperature dependence on SZA is weak then we can proceed under the assumptions made for Figures 7 and 8. However, if we find that the electron temperature dependence on SZA is strong then we will first need to account for this dependence

– possibly by fitting the SZA dependence with an analytical function and normalizing the electron temperatures to one representative SZA. Though our ultimate goal is to understand the effects of crustal magnetic fields on the Martian ionosphere, establishing how the electron temperature changes with SZA would represent an extremely valuable scientific result in its own right.

Along with controlling for changes in factors like season, solar flux, and spatial coverage, we will perform statistical significance tests to assess the validity of our results. For example, we can quantify the variability of the electron density in a specific spatial (altitude/latitude/longitude) region and compare it to how much the median or average electron density is enhanced in regions of strong crustal fields compared to regions of weak crustal fields. If we find that the variability is small compared to the crustal field enhancement then we can conclude that the crustal field effects are significant.

Expected significance: The results of Task B will establish for the first time how crustal fields influence the ion composition and electron temperatures in the dayside Martian ionosphere. In the course of our analysis we will also establish how the electron temperature in the dayside ionosphere varies with solar zenith angle. Our findings will also provide the first detailed study of how crustal fields influence the electron density at low altitudes (< ~300 km). This information, in turn, will help improve our understanding of how Mars' unique magnetic field environment influences the structure of the ionosphere, an important step toward understanding crustal fields influence the planetary interaction with the solar wind and processes that can lead to atmospheric escape to space. We intend to publish our findings in at least one paper in a peer-reviewed journal.

3.3 Task C: Modeling study to interpret effects of crustal fields on the ionosphere

The final task is modeling work to help interpret the results of Tasks A and B. We will use the BU Mars Ionosphere Model, which was used by *Matta et al.* [2015] to study field-aligned vertical and horizontal plasma transport in regions of strong crustal fields.

Matta et al. [2015] describe the model as follows: "The BU Mars Ionosphere Model is a fluid model that solves for photochemical production and loss as well as plasma transport in the ionosphere between the lower and upper boundaries of 80 and 400 km, respectively, while conserving mass and momentum [*Matta*, 2013]. … [T]he model was expanded from one (vertical) into two (vertical and meridional) spatial dimensions to incorporate the effects of vertical as well as horizontal plasma transport in a region spanning ~20° in latitude." The model uses a "simplified chemical scheme … that produces five ions (CO_2^+, O_2^+, O^+, CO^+, and NO^+) [e.g., *Martinis et al*., 2003; *Mendillo et al.*, 2011] with full transport physics [e.g., *Matta et al.*, 2013, 2014]. … The model takes as input a diurnally fixed neutral atmosphere derived from lower boundary (homopause) mixing ratios of CO_2, O, CO, Ar, N_2, and H_2 taken from the Mars Climate Database (version 5.1) using solar minimum conditions at 120–150° solar longitude, 42°S latitude and 15°E longitude [*Forget et al.*, 1999; *Lewis et al.*, 1999; *Millour et al.*, 2014]. … Plasma temperatures are derived from Viking Lander 1 measurements [*Hanson et al.*, 1977; *Hanson and Mantas*, 1988], with the electron temperature extrapolated downward and adjusted for local conditions as described in *Mendillo et al.* [2011]. A slice along the meridian of the magnetic field morphology representative of a strong crustal magnetic field region was then used to investigate plasma dynamics in the ionosphere … The boundary conditions used in the model simulations are similar to those described in previous works [e.g., Mendillo et al., 2011; Matta et al., 2013, 2014]. In summary, no transport occurs at the lower boundary, and the upper boundary

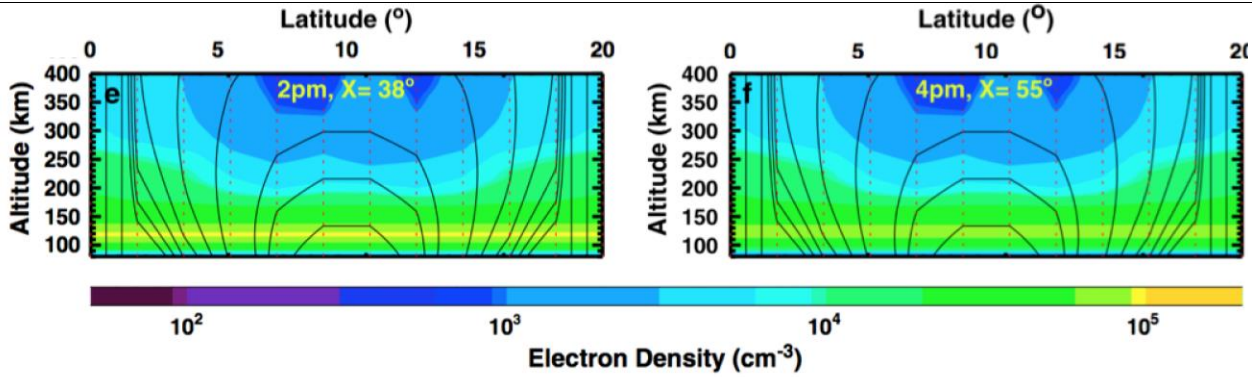

Figure 9. Simulated electron density maps in regions of strong crustal fields, shown for two local times. Modified from *Matta et al.* [2015], figure 2.

is constrained such that at every topside horizontal grid, ion densities decrease exponentially with a fixed plasma scale height determined by zero velocity conditions. No plasma drifts through the left or right edges of the simulation region due to the imposed vertical field line structure at those boundaries."

Matta et al. [2015] approximated the magnetic field in the simulation region using a dipole magnetic field placed 100 km below the surface. This provided good agreement with the crustal field model of *Arkani-Hamed* [2004] in the simulation region and included closed arcade-like loop field lines and open field lines at the edge of the simulation region (see Figure 9). They then ran the model for a Martian day, calculating the ionospheric density in time steps of 0.8s. The model incorporates chemical production and loss and solves the ion and electron equation of motion that incorporates the Lorentz force, the polarization electric field that produces charge neutrality, plasma pressure gradients, gravity, and collisions. The model outputs are ion and electron densities as a function of space and time.

Model results from two dayside local times are shown in Figure 9. The model predicts a non-uniform density structure with latitude at altitudes above the main peak at ~130 km. At a given altitude densities are largest at the edges of the simulation box, where the field lines are vertical, and smallest where the field lines are horizontal at the center of the simulation region. At the highest altitudes the density is most depleted at intermediate latitudes where the field is not purely horizontal or purely vertical. *Matta et al.* [2015] suggested that the ionosphere is most inflated in regions of vertical field because plasma at lower altitudes can easily diffuse upward. They noted that there is a larger plasma pressure in open field regions and therefore the boundary between the solar wind and the ionosphere should be at higher altitudes in open field regions than in other areas, which is consistent with MGS observations [*Mitchell et al.*, 2001].

We propose to update and expand the model of *Matta et al.* [2015] so that model results can be compared to the MAVEN observations analyzed in Tasks A and B. Specifically, we will update the model to cover a larger spatial region and incorporate a more realistic magnetic field geometry, neutral atmosphere, and electron temperatures. **The goal of this modeling work is to understand the effects of the crustal magnetic fields on plasma transport.** In Task A we will use MAVEN observations to determine whether there is observational evidence that solar wind interactions with crustal fields lead to changes in the structure of the ionosphere, and specifically whether plasma heating by the solar wind can influence the electron density. In this modeling work we will neglect the role of the solar wind and will test the effects of plasma transport alone.

We will fly a virtual spacecraft through the model region to perform detailed comparisons between the predicted and observed electron densities and ion composition along a handful of MAVEN orbits in a region of strong crustal fields (orbits from fall 2015 as in Task A). In cases where the model and observations agree we can conclude that plasma transport can explain any observed changes in the ionospheric structure. In cases where the model and observations disagree we can conclude that other physical processes, possibly heating by the solar wind, must be at work.

Expanding the model's spatial coverage is important so that model output can be compared to the MAVEN observations from fall 2015 that will be analyzed in Task A. For example, the orbital tracks in Figure 4 show that MAVEN's orbit covers ~30º of latitude at ionospheric altitudes, while the current model only covers 20º latitude. As the model is applied to a larger spatial region it will also become necessary to incorporate a more realistic magnetic field geometry. The current model implementation includes only one closed crustal field loop (see Figure 9). However, in our observations the spacecraft goes through multiple cusp regions and more than one closed magnetic field loop, as evidenced by both the multiple zero crossings of B_r, the radial component of the magnetic field, in Figure 5 and by comparing the MAVEN orbit tracks in Figure 4 to regions of alternating B_r polarity in figure 1. Therefore we intend to incorporate a more realistic magnetic field model in our proposed simulations. Several models have been developed using the MGS observations to describe the crustal magnetic fields at altitudes as low as the surface [e.g. *Arkani-Hamed*, 2001, 2004; *Cain et al.*, 2003; *Morschhauser et al.*, 2014], and we will use one of these models (or a simplified version) in our simulation.

From Task B we will have quantified how properties like the electron density, temperature, and ion composition change globally in response to regions of strong crustal field magnitude and regions of strongly vertical or strongly horizontal crustal magnetic field. We will compare the observational results of Task B to our modeling outputs in addition to performing detailed comparisons between the model and individual orbits from Task A. Comparing the modeling results to a global survey will provide useful insights into the overall effects of crustal fields on a larger scale. In order to provide a useful comparison between the modeled and observed changes in ion composition and electron temperatures it is important to begin with a background neutral atmosphere and electron temperatures that accurately reflect the observed values. Prior to MAVEN, the only measurements of these quantities were single profiles from Viking, at a single solar zenith angle, which have been shown to differ from the more recent MAVEN observations [*Ergun et al.*, 2015; *Withers et al.*, 2015]. We will update the model to include a more realistic neutral atmosphere and more realistic electron temperatures.

Expected significance: The results of this modeling work will help quantify how crustal fields can influence the structure of the ionosphere through plasma transport, one possible physical mechanism through which crustal fields can influence the ionosphere. By comparing model outputs to observations we can identify cases in which other physical processes, like plasma heating by the solar wind, may be more important. We intend to publish our findings in a peer-reviewed journal. We expect the modeling work will be published as a stand-alone study but it could also be partly incorporated into papers describing the results of Tasks A and B.

4. Research team and work plan

PI Marissa Vogt will be responsible for the management of this investigation and compliance with all reporting requirements. PI Vogt will also be responsible for the day-to-day work for the project, interactions with the undergraduate student, and completion of the data management plan. She has been a member of the MAVEN science team since early 2014 and has published studies of the Martian ionosphere using MAVEN data [*Vogt et al.*, 2015, 2016].

Co-I Majd Mayyasi (formerly Matta) will perform the modeling work described in Task C. Her Ph.D. thesis work involved modeling the Martian ionosphere using the BU Mars Ionosphere Model [*Matta*, 2013] and she has used an expanded version of the model to investigate the effects of crustal fields on the ionosphere [*Matta et al.*, 2015].

Co-I Paul Withers will advise on the MAVEN data analysis and modeling work. He is a leading expert on the dayside Martian ionosphere [e.g. *Withers*, 2009] and has studied the effects of crustal fields on radio occultation measurements at Mars [*Withers et al.*, 2005].

A Boston University undergraduate student will assist with the data analysis in Tasks A and B and modeling work in Task C. Our preferred candidate for this work is Casey Flynn, an undergraduate who has worked with us since summer 2015 and will graduate in 2018. She performed the initial analysis shown in Figures 7 and 8 under the supervision of Dr. Vogt and Professor Withers. After Casey graduates we will recruit a new undergraduate student.

Our work plan is as follows: in **year 1** PI Vogt, assisted by Co-I Withers and the undergraduate student, will perform the analysis for **Task A** (3 months) and write up a manuscript describing the results (1 month). Also in **year 1**, Co-I Mayyasi will modify the BU Mars Ionosphere Model to cover a larger spatial region and more realistic magnetic field and neutral atmosphere (3 months) and will begin modifying the model to incorporate more realistic electron temperatures (1 month).

In **years 2 and 3** PI Vogt, assisted by Co-I Withers and the undergraduate student, will perform the analysis for **Task B**, including an initial survey of the electron temperature changes with solar zenith angle (2 months) and analysis of how various ionospheric properties change with latitude and longitude, controlling for variables like seasons and solar ionizing flux (3 months). The team will also write up a manuscript describing the results of **Task B** (1 month). For **Task C**, Co-I Mayyasi will use the results of Tasks A and B to complete modifying the model to incorporate more realistic electron temperatures (1 month). Co-I Mayyasi will then perform simulations for comparison to data from specific MAVEN orbits from Task A (2 months) and for comparison to the global survey of MAVEN observations from Task B (4 months). Co-I Mayyasi will write up a manuscript describing the results of the modeling work in **Task C** (1 month). PI Vogt, along with Co-I Withers and the undergraduate student, will assist Co-I Mayyasi in comparing model outputs from Task C to the results of Tasks A and B and in writing the manuscript (2 months).

5. Statement of Relevance

This work is relevant to the Mars Data Analysis Program because it will involve analysis of data from MAVEN, a NASA Mars mission, and will use model results to interpret the data. Our work will help "[c]onstrain the processes that control the chemical composition of the atmosphere and surrounding plasma environment", which is one of the objectives outlined in the MEPAG Science Goals 2015 document (http://mepag.jpl.nasa.gov).

6. Statement of non-overlap with current funding or mission responsibilities

PI Vogt, Co-I Mayyasi, and Co-I Withers are all members of the MAVEN science team. However, the work described in this proposal does not overlap with any of the data analysis or responsibilities that are currently funded by NASA through the MAVEN project. PI Vogt was funded through Co-I Withers' MAVEN Participating Scientist (PS) grant but is now (as of April 2016) funded entirely by an NSF postdoctoral fellowship on the topic of Jupiter's magnetosphere. Because PI Vogt's funding no longer comes from the MAVEN project we have requested funds to support her travel to 2 MAVEN science team meetings (PSG meetings) per year, as described in the budget justification. Co-I Withers' MAVEN PS grant ended in September 2016. His continued MAVEN funding is for the acquisition of new MAVEN radio occultation observations, which are not included in this proposed work. Co-I Mayyasi is a member of MAVEN's IUVS instrument team and her funding is related to IUVS data analysis and reduction, but IUVS data are not part of the work proposed here. Therefore, though Co-Is Withers and Mayyasi both already receive some funding from NASA through the MAVEN project, the work described in this proposal does not contain any overlap with their current funding or mission responsibilities.

References

Andersson, L., R. E. Ergun, G. T. Delory, A. Eriksson, J. Westfall, H. Reed, J. McCauly, D. Summers, *and* D. Meyers (2015), The Langmuir probe and waves (LPW) instrument for MAVEN, *Space Sci. Rev., doi:10.1007/s11214-015-0194-3.*

Andrews, D. J., N. J. T. Edberg, A. I. Eriksson, D. A. Gurnett, D. Morgan, F. Němec, and H. J. Opgenoorth (2015a), Control of the topside Martian ionosphere by crustal magnetic fields, *J. Geophys. Res. Space Physics*, *120*, 3042–3058, doi:10.1002/2014JA020703.

Andrews, D. J., L. Andersson, G. T. Delory, R. E. Ergun, A. I. Eriksson, C. M. Fowler, T. McEnulty, M. W. Morooka, T. Weber, and B. M. Jakosky (2015b), Ionospheric plasma density variations observed at Mars by MAVEN/LPW, *Geophys. Res. Lett.*, *42*, doi:10.1002/2015GL065241.

Arkani-Hamed, J. (2001), A 50 degree spherical harmonic model of the magnetic field of Mars, *J. Geophys. Res.*, *106*, 23,197–23,208, doi:10.1029/2000JE001365.

Cain, J. C., B. B. Ferguson, and D. Mozzoni (2003), An n = 90 internal potential function of the Martian crustal magnetic field, *J. Geophys. Res.*, *108*, 5008, doi:10.1029/2000JE001487, E2.

Chamberlin, P. C., T. N. Woods, and F. G. Eparvier (2007), Flare irradiance spectral model (FISM): Daily component algorithms and results, *Space Weather*, 5, S07005, doi:10.1029/2007SW000316.

Chamberlin, P. C., T. N. Woods, and F. G. Eparvier (2008), Flare irradiance spectral model (FISM): Flare component algorithms and results, *Space Weather*, 6, S05001, doi:10.1029/2007SW000372.

Connerney, J. E. P., M. H. Acuña, P. J. Wasilewski, G. Kletetschka, N. F. Ness, H. Rème, R. P. Lin, and D. L. Mitchell (2001), The global magnetic field of Mars and implications for crustal evolution, *Geophys. Res. Lett.*, *28*, 4015-4018, doi:10.1029/2001GL013619.

Connerney, J. E. P., J. Espley, P. Lawton, S. Murphy, J. Odom, R. Oliversen, and D. Sheppard (2015), The MAVEN magnetic field investigation, *Space Sci. Rev.*, doi:10.1007/s11214-015-0169-4.

Edberg, N. J. T., M. Lester, S. W. H. Cowley, and A. I. Eriksson (2008), Statistical analysis of the location of the Martian magnetic pileup boundary and bow shock and the influence of crustal magnetic fields, *J. Geophys. Res.*, *113*, A08206, doi:10.1029/2008JA013096.

Eparvier, F. G., P. C. Chamberlin, T. N. Woods, and E. M. B. Thiemann (2015), The solar extreme ultraviolet monitor for MAVEN, *Space Science Reviews*, 1-9, doi:10.1007/s11214-015-0195-2.

Ergun, R. E., M. W. Morooka, L. A. Andersson, C. M. Fowler, G. T. Delory, D. J. Andrews, A. I. Eriksson, T. McEnulty, and B. M. Jakosky (2015), Dayside electron temperature and density profiles at Mars: First results from the MAVEN Langmuir probe and waves instrument, *Geophys. Res. Lett*., 42, 8846–8853, doi:10.1002/2015GL065280.

Fallows, K., P. Withers, and M. Matta (2015), Numerical simulations of the influence of solar zenith angle on properties of the M1 layer of the Mars ionosphere, *J. Geophys. Res. Space Physics*, *120*, doi:10.1002/2014JA020947.

Fillingim, M. O., R. J. Lillis, S. L. England, L. M. Peticolas, D. A. Brain, J. S. Halekas, C. Paty, D. Lummerzheim, and S. W. Bougher (2012), On wind-driven electrojets at magnetic cusps in the nightside ionosphere of Mars, *Earth Planets Space*, 64, 93–103.

Forget, F., F. Hourdin, R. Fournier, C. Hourdin, O. Talagrand, M. Collins, S. R. Lewis, P. L. Read, and J.-P. Huot (1999), Improved general circulation models of the Martian atmosphere from the surface to above 80 km, *J. Geophys. Res.*, *104*, 24,155–24,176, doi:10.1029/1999JE001025.

Fox, J. L. (2004), Response of the Martian thermosphere/ionosphere to enhanced fluxes of solar soft X rays, *J. Geophys. Res.*, *109*, A11310, doi:10.1029/2004JA010380.

Gurnett, D. A., R. L. Huff, D. D. Morgan, A. M. Persoon, T. F. Averkamp, D. L. Kirchner, F. Duru, F. Akalin, A. J. Kopf, E. Nielsen, A. Safaeinili, J. J. Plaut, and G. Picardi (2008), An overview of radar soundings of the Martian ionosphere from the Mars Express spacecraft, *Adv. Space Res.*, *41*, 1335-1346, doi:10.1016/j.asr.2007.01.062.

Halekas, J. S., E. R. Taylor, G. Dalton, G. Johnson, D. W. Curtis, J. P. McFadden, D. L. Mitchell, R. P. Lin, and B. M. Jakosky (2014), The solar wind ion analyzer for MAVEN, *Space Sci. Rev.*, doi:10.1007/s11214-013-0029-z.

Hanson, W. B., and G. P. Mantas (1988), Viking electron temperature measurements: Evidence for a magnetic field in the Martian ionosphere, *J. Geophys. Res.*, 93(A7), 7538–7544.

Hanson, W.B., S. Sanatani, and D. R. Zuccaro (1977), The Martian ionosphere as observed by the Viking retarding potential analyzers, *J. Geophys. Res.*, *82*, 4351–4363.

Jakosky, B. M., et al., 2015, The Mars Atmosphere and Volatile Evolution (MAVEN) Mission, *Space Sci. Rev.*, 10.1007/s11214-015-0139-x.

Lewis, S. R., M. Collins, P. L. Read, F. Forget, F. Hourdin, R. Fournier, C. Hourdin, O. Talagrand, and J.-P. Huot (1999), A climate database for Mars, *J. Geophys. Res.*, *104*, 24,177–24,194, doi:10.1029/1999JE001024.

Ma, Y., A. F. Nagy, K. C. Hansen, D. L. DeZeeuw, T. I. Gombosi, and K. G. Powell (2002), Three-dimensional multispecies MHD studies of the solar wind interaction with Mars in the presence of crustal fields, *J. Geophys. Res.*, *107*(A10), 1282, doi:10.1029/2002JA009293.

Mahaffy, P. R., et al. (2014), The neutral gas and ion mass spectrometer on the Mars atmosphere and volatile evolution mission, *Space Sci. Rev.*, doi:10.1007/s11214-014-0091-1.

Martinis, C. R., J. K. Wilson, *and* M. J. Mendillo (2003), Modeling day-to-day ionospheric variability on Mars, *J. Geophys. Res.,* 108, 1383, *doi:10.1029/2003JA009973.*

Matta, M. M. (2013), Modeling the Martian Ionosphere, PhD Thesis, Boston Univ., Boston, Mass.

Matta, M., P. Withers, M. Mendillo (2013), The Composition of Mars' Topside Ionosphere: Effects of Hydrogen, *J. Geophys. Res.*, *118*, p. 2681-2693, doi: 10.1002/jgra.50104.

Matta, M., M. Galand, L. Moore, M. Mendillo, and P. Withers (2014), Numerical simulations of ion and electron temperatures in the ionosphere of Mars: Multiple ions and diurnal variations, *Icarus*, 227, 78–88, doi:10.1016/j.icarus.2013.09.006.

Matta, M., M. Mendillo, P. Withers, and D. Morgan (2015), Interpreting Mars ionospheric anomalies over crustal magnetic field regions using a 2-D ionospheric model, *J. Geophys. Res. Space Physics*, *120*, 766–777, doi:10.1002/2014JA020721.

McFadden, J. P., O. Kortmann, D. Curtis, G. Dalton, G. Johnson, R. Abiad, R. Sterling, K. Hatch, P. Berg, C. Tiu, D. Gordon, S. Heavner, M. Robinson, M. Marckwordt, R. Lin, and B. Jakosky (2015), MAVEN Suprathermal and Thermal Ion Composition (STATIC) Instrument, *Space Sci. Rev.*, *195*: 199. doi:10.1007/s11214-015-0175-6.

Mendillo, M., A. Lollo, P. Withers, M. Matta, M. Pätzold, and S. Tellmann (2011), Modeling Mars' ionosphere with constraints from same-day observations by Mars Global Surveyor and Mars Express, *J. Geophys. Res.*, *116*, A11303, doi:10.1029/2011JA016865.

Millour, E., et al. (2014), The Mars climate database, Eighth Int. Conf. Mars, 1791, p. 1184, 2014LPICo1791.1184M.

Mitchell, D. L., R. P. Lin, C. Mazelle, H. Rème, P. A. Cloutier, J. E. P. Connerney, M. H. Acuña, and N. F. Ness (2001), Probing Mars' crustal magnetic field and ionosphere with the MGS Electron Reflectometer, *J. Geophys. Res*., *106*(E10), 23,419–23,428, doi:10.1029/2000JE001435.

Nielsen, E., M. Fraenz, H. Zou, J.-S. Wang, D. A. Gurnett, D. L. Kirchner, D. D. Morgan, R. Huff, A. Safaeinili, J. J. Plaut, G. Picardi, J. D. Winningham, R. A. Frahm, and R. Lundin, (2007) Local plasma processes and enhanced electron densities in the lower ionosphere in magnetic cusp regions on Mars, *Planet. Space Sci.*, *55*, 2164–217, doi:10.1016/j.pss.2007.07.003.

Riousset, J. A., C. S. Paty, R. J. Lillis, M. O. Fillingim, S. L. England, P. G. Withers, and J. P. M. Hale (2014), Electrodynamics of the Martian dynamo region near magnetic cusps and loops, *Geophys. Res. Lett*., *41*, 1119–1125, doi:10.1002/2013GL059130.

Schunk, R. W., and A. F. Nagy (2009), Ionospheres, 2nd ed., Cambridge Univ. Press, New York.

Vogt, M. F., P. Withers, P. R. Mahaffy, M. Benna, M. K. Elrod, J. S. Halekas, J. E. P. Connerney, J. R. Espley, D. L. Mitchell, C. Mazelle, and B. M. Jakosky (2015), Ionopause-like density gradients in the Martian ionosphere: A first look with MAVEN, *Geophys. Res. Lett.*, *42*, doi:10.1002/2015GL065269.

Vogt, M. F., P. Withers, K. Fallows, C. L. Flynn, D. J. Andrews, F. Duru, and D. D. Morgan (2016), Electron densities in the ionosphere of Mars: A comparison of MARSIS and radio occultation measurements, *J. Geophys. Res. Space Physics*, *121*, doi:10.1002/2016JA022987.

Withers, P. (2009), A review of observed variability in the dayside ionosphere of Mars, *Adv. in Space Res.*, *44*, 277-307, doi:10.1016/j.asr.2009.04.027
Withers, P., M. J. Mendillo, H. Rishbeth, D. P. Hinson, and J. Arkani-Hamed (2005), Ionospheric characteristics above Martian crustal magnetic anomalies, Geophys. Res. Lett., 32, L16204, doi:10.1029/2005GL023483.

Withers, P., K. Fallows, and M. Matta (2014), Predictions of electron temperatures in the Mars ionosphere and their effects on electron densities, *Geophys. Res. Lett.,* 41, 2681–2686, *doi:10.1002/2014GL059683.*

Withers, P., M. F. Vogt, P. R. Mahaffy, M. Benna, M. K. Elrod, and B. M. Jakosky (2015), Changes in the thermosphere and ionosphere of Mars from Viking to MAVEN, *Geophys. Res. Lett*., *42*, doi:10.1002/2015GL065985.